

A Dynamical Characterization of Internally-Actuated Microgravity Mobility Systems

Adam W. Koenig, Marco Pavone, Julie C. Castillo-Rogez, Issa A. D. Nenas

Abstract—The *in-situ* exploration of small Solar System bodies (such as asteroids or comets) is becoming a central objective for future planetary exploration. Such bodies are characterized by very weak gravitational fields, which make hopping mobility platforms one of the preferred mobility strategies for microgravity surface exploration, as recognized by space agencies worldwide. However, little is known about the dynamical behavior of hopping platforms in low gravity environments, where small bodies’ rotational dynamics can have a critical effect. Accordingly, the objective of this paper is to study in detail the “dynamic envelope” of hopping microgravity rovers, with a focus on internal actuation. Specifically, we first perform a static analysis with the goal of determining regions of a small body where an internally-actuated hopping rover can stably stay at rest. Then, we perform a dynamic analysis and discuss the performance of hopping microgravity platforms as a function of a number of system and environmental parameters (e.g., body rotation rate) and in terms of a number of mobility aspects (e.g., initial hopping angles, ballistic flight, and rebounding dynamics). Finally, we tailor our analysis to a potential mission to Mars’ moon Phobos. Collectively, our results show that internally-actuated rovers, when designed according to the guidelines developed in this paper, are a viable mobility solution for a vast class of small Solar System bodies. Also, our analysis represents a key first step to develop path planning algorithms for microgravity explorers to safely explore dynamically feasible regions.

I. INTRODUCTION

The *in-situ* exploration of small Solar System bodies (such as asteroids, comets, or irregular satellites) is becoming a central objective for future planetary exploration [1], [5]. The primary scientific return of such missions would be the characterization of planetary material composition and chemistry, which holds the promise of shedding light on the origin and dynamical evolution of the Solar System [5]. Furthermore, such missions, by characterizing regolith mechanical properties, dust dynamics, and electrostatic charging, could pave the way for Human Exploration in the Solar System [18]. However, weak gravitational fields (micro-g to milli-g), which are characteristic of small bodies, make the development of microgravity robotic explorers a challenge,

Adam W. Koenig and Marco Pavone are with the Department of Aeronautics and Astronautics, Stanford University, Stanford, CA 94305 {awkoenig, pavone}@stanford.edu.

Julie C. Castillo-Rogez and Issa A. D. Nenas are with the Jet Propulsion Laboratory, California Institute of Technology, Pasadena, CA 91109 {julie.c.castillo, issa.a.nenas}@jpl.nasa.gov.

*The research described in this paper was partially carried out at the Jet Propulsion Laboratory (JPL), California Institute of Technology, and was partially supported by JPL under the R&TD and CIF programs. The authors wish to acknowledge insightful discussions with Dr. Cinzia Zuffada (JPL), Dr. Tom Cwik (JPL), and Dr. Jonas Zmuidzinis (JPL). Government sponsorship acknowledged.

and the selection of the “best” mobility mechanism for *controlled* mobility on small bodies is an open problem.

Essentially, mobility mechanisms for micro-gravity environments can be broadly divided into four classes, namely, mobility via thrusters, wheeled mobility, legged mobility, and hopping mobility. In the absence of strong traction forces, wheeled vehicles are limited to extremely low speeds (1.5 mm/s per previous JPL studies [10]). Use of thrusters poses risk of surface contamination, negatively affecting the science return of the mission. Additionally, thrusters are characterized by mechanical and operational complexity, and their lifetime is critically limited by propellant availability. Legged mobility systems are also characterized by mechanical complexity. Furthermore, contact forces between legs and the surface vary widely with surface characteristics, which cannot be accurately determined beforehand. Hopping systems use the low gravity levels to their advantage. Prototypes of hopping systems have been developed by several agencies including NASA [10], [7], RKA [14], ESA [6], and JAXA [2]. There are two types of hopping designs: (#1) the rover drives an external contact point into the ground [7], [17], and (#2) the hopper develops internal momentum to augment contact forces [19], [11]. Key advantages of hopping platforms include relatively simple actuation, ability to cover a large surface, and relative insensitivity to soil characteristics. Additionally, internally-actuated systems possess the key advantages of immunity to contamination from surface dust and simplified thermal control.

Despite the apparent consensus about the advantages of hopping platforms for small bodies exploration, little is known about their dynamical behavior in low gravity environments, where small bodies’ rotational dynamics can have a critical effect. Consider, for example, a small spherical body of uniform density. Depending on the class of asteroid, density can range from approximately 1 g/cm^3 to 6 g/cm^3 . Using Newton’s formula for gravitational acceleration, one can estimate the gravity on the surface of a uniform spherical body according to $a_g = 4G\pi\rho r/3$, where ρ is the (constant) object’s density, G is the gravitational constant, and r is the radius of the body. Now, assume that the body is rotating. At the equatorial position, the observed surface acceleration is reduced by the centripetal acceleration, denoted by a_c . To ensure that the rover stays in contact with the body, one needs $a_c \leq a_g$ which translates into a bound for the body’s angular velocity reading as $\omega \leq \sqrt{4G\pi\rho/3}$. Considering the aforementioned typical values for asteroids’ density, one obtains maximum values for the angular velocity in the range $5 \cdot 10^{-4} \text{ rad/s}$ to 10^{-3} rad/s , which have been

observed for known bodies. These considerations call for an in-depth assessment of the “dynamic envelope” of hopping microgravity explorers. To the best of our knowledge, only two studies have (partially) addressed this problem. In [9], the authors study the stability of different points on a rotating ellipsoid, while in [4] the authors consider the effect of friction on a point mass bouncing on a rotating ellipsoid. These studies, however, do not treat the rovers as rigid bodies and do not take into account actuation mechanisms, and therefore their relevance to rover’s design and path planning appears limited.

Accordingly, the objective of this paper is to study in detail the “dynamic envelope” of hopping microgravity rovers, with a focus on internal actuation (part of our analysis, however, is also applicable to other types of rovers not equipped with gripping mechanisms, such as externally-actuated hoppers and wheeled vehicles). In particular, the contribution of this paper is threefold. First, we present a *static analysis* that allows determination of the regions of a small body where an internally-actuated hopping rover (and indeed any rover not equipped with thrusters or gripping mechanisms) can stably stay at rest, e.g., to recharge the batteries or to acquire measurements. Second (this is the main contribution of the paper), we present a *dynamic analysis* of internally-actuated hopping platforms and discuss their performance as a function of a number of system and environmental parameters (e.g., rover shape), and in terms of a number of mobility aspects (e.g., initial hopping angles, ballistic flight, rebounding dynamics, and instrument pointing). Finally, we tailor our analysis to a potential mission to Mars’ moon Phobos. Collectively, our results show that internally-actuated rovers, from a dynamic standpoint, are a viable mobility solution for a vast class of small Solar System bodies. Also, our analysis represents a key first step to develop path planning algorithms for microgravity explorers to safely explore dynamically feasible regions.

The rest of the paper is structured as follows. In Section II we discuss the mathematical models for the hopping rover and the environment. In Section III we present the static analysis, while in Section IV we present the dynamic analysis. Then, in Section V we discuss the results for a case study for Mars’ moon Phobos and briefly consider similar bodies. Finally, in Section VI we summarize our findings and discuss direction for future work.

II. MODELS FOR THE ROVER AND THE ENVIRONMENT

In this section we present the mathematical model for the rovers we wish to study and our assumptions about the environment.

A. Geometrical and Actuation Model for the Rover

We model a microgravity hopper as a rigid body with mass m , to which a set of n mass-less spikes are attached. It is assumed that the tips of the spikes constitute the vertices of a convex polyhedron. The tip of each spike is located a distance l_i from the center of mass and is oriented at an angle θ_i from the surface normal vector \hat{n} .

The rover is *internally-actuated* through a set of actuators that develop internal *linear* or *angular* momentum to temporarily augment contact forces. *Linear actuators* consist of a mass constrained to move along an axis actuated by a linear motor. To reduce power requirements of the motor, the system may use the motor to stretch a spring, which is then released to actuate the rover. *Angular actuators* consist of a flywheel and a rotary motor. This system can be implemented using a very small motor to spin up the flywheel, after which a braking mechanism or similar system quickly decelerates the flywheel, actuating the rover. Both linear and angular systems can be implemented with multiple actuators on different axes used together or a single actuator on a rotating frame to develop momentum in any direction.

B. Environmental Model

A small body is modeled as a (possibly non-convex) polyhedron, where the local normal to a face is indicated by \hat{n} . We make the natural assumption that its angular velocity vector $\vec{\omega}$ and angular acceleration vector $\vec{\alpha}$ have independent magnitudes lying in a bounded set. We also assume that the density of the object is uniform, so that the local gravity field can be computed knowing only its mass and shape when empirical models are not available.

Contact forces from each spike in contact with the surface can be divided into two components: the component normal to the surface, \vec{F}_{N_i} , and the component tangent to the surface, \vec{F}_{f_i} , where i is the index of a spike in contact with the surface. In this paper we consider a Coulomb friction model to calculate contact forces on each spike, which reads as:

$$\begin{cases} \|\vec{F}_{f_i}\| \leq \mu_s \|\vec{F}_{N_i}\| & \text{if } \vec{v}_i = 0, \\ \|\vec{F}_{f_i}\| = \mu_k \|\vec{F}_{N_i}\|, & \text{if } \vec{v}_i \neq 0, \end{cases}$$

where v_i is the relative velocity between the tip of the i th spike and the surface, μ_s is the coefficient of static friction, and μ_k is the coefficient of kinetic friction.

C. Model Generality

Our model of internally-actuated rovers captures a large variety of existing prototypes, including MINERVA, the Hedgehog, MASCOT, and Cubli (developed for Earth gravity applications), see Figure 1.

As discussed, our model assumes that the small body has uniform density; indeed, our results can be easily generalized to the nonuniform case whenever the gravitational field is known. Our assumption of a Coulomb friction model is more problematic, since the Coulomb model is known to be quite inaccurate for slipping interactions with small particulate surfaces. We note, however, that this model usually yields first-order analyses of rover mobility well matched by experiments [20], so we believe this is sufficient for the first-order static and dynamic analyses performed in this paper. Finally, our assumption of a locally flat surface can be scaled to the limits of our knowledge of a target small body. We recognize that the existence of small geographic features may impact

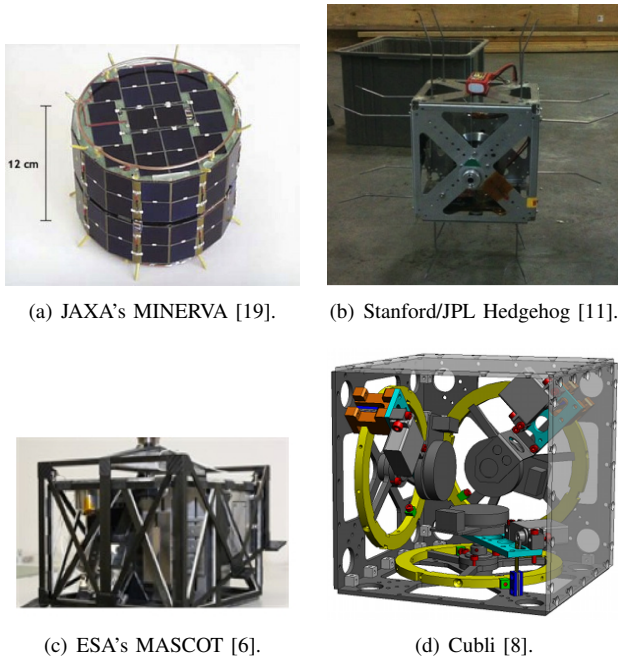


Fig. 1. Examples of internally-actuated rovers that can be studied within the framework presented in this paper. All four platforms have angular actuators inside the enclosure.

mobility, but these features have little impact on a global feasibility study as presented here.

III. STATIC ANALYSIS

In this section we study the passive stability of internally-actuated rovers on small Solar System bodies (potentially undergoing a rotational motion). This analysis allows us to identify regions where such rovers could safely land and/or stably stay at rest for either battery re-charging or measurement acquisition.

A. Governing Equations

According to Newton's laws, the three conditions that must be satisfied by a rover to be at rest on the surface of a rotating body read as follows:

- 1) $\sum \vec{F}_{N_i} + \sum \vec{F}_{f_i} + m\vec{g} = m(\vec{\omega} \times \vec{\omega} \times \vec{r} + \vec{\alpha} \times \vec{r})$,
- 2) $\|\sum \vec{F}_{f_i}\| / \|\sum \vec{F}_{N_i}\| \leq \min(\mu_s, \tan(\phi))$,
- 3) $\vec{F}_{N_i} \cdot \hat{n} \geq 0$,

where i is the index for the spikes in contact with the terrain, \vec{r} is the vector from the body center of mass to the (locally flat) surface where the rover stands, and ϕ is the maximum angle the rover can be tipped before it will continue to roll. This angle is defined in any direction by the polygon formed by spikes in contact with the surface, hereafter called the support polygon. The first equation defines the unique total contact force required to stay in place. The second condition requires that the rover does not slip or roll. The third relation enforces the no-grip stipulation.

B. Numerical Procedure

The aim of the static analysis is to determine whether the three aforementioned conditions are met for a given

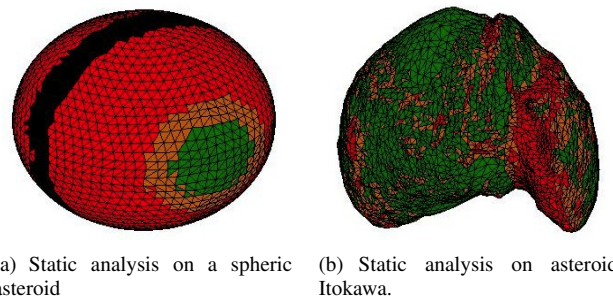


Fig. 2. Static analysis for two representative small bodies.

rover shape and rotating body. The shape of the body is assumed to be known from radar or other measurements and is treated as a polyhedron (see Section II). If no empirical gravity field is available, one can be calculated from the mass and shape of the body under the assumption of uniform density. Specifically, one discretizes the mass into a grid of specified resolution, gives each interior point in the grid an equal mass, and sums the contributions of each mass at each point of interest. To account for the effects of rotation, the boundary of the set of possible angular velocities and accelerations is sampled and used to compute centripetal and Euler acceleration. Because the transformations from angular velocity and acceleration to their corresponding Euclidean accelerations are continuous, if any rotational state exists that causes these conditions to be violated, there must exist a state on the boundary of the set that violates the same conditions. We take advantage of this by only sampling the boundary of the set of rotational values, saving computation time. To determine passive stability, the necessary contact force to achieve static equilibrium is calculated at all points of interest on the body for each rotational state considered. If the face is stable, this contact force will satisfy the above conditions.

C. Numerical Experiments

In this section we aim to illustrate the effects of body geometry and rotation on the existence of passively stable regions. The aforementioned analysis has been implemented on a spherical body (selected solely to illustrate rotation effects), and the asteroid Itokawa. The sphere has density 5 g/cm^3 , is rotating at 0.0012 rad/sec , and has a presumed static friction coefficient of 0.7. We consider a Hedgehog shaped rover (spikes defining orthogonal octagons) with mass 10 kg and spike length of 0.2 m [11]. The results are shown in Figure 2(a). One can distinguish four different regions. Specifically, the green region represents the part of the asteroid where the system can stably stay at rest and the orange region denotes regions where the rover would roll without slipping, which depends *only* on the selected geometry. The red region represents the part of the asteroid where the rover will slip, but remain on the surface and the black region is where the rover would be thrown from the surface. No system without gripping or thruster capability could stay at rest in the red or black regions.

Figure 2(b) shows a similar analysis for the asteroid Itokawa, which has mass $3.56 \cdot 10^{10}$ kg, a presumed static friction coefficient of 0.7, and is rotating with a period of 12 hours. One can observe that a hopping rover could stably stay at rest on most regions on Itokawa.

D. Implications for System Design and Mission Feasibility

The results in this section and presented later in Table I suggest that internally-actuated rovers can stably operate on scientifically interesting small bodies, such as Itokawa. The presence of the orange regions suggests that more regions on these bodies would be explorable if the selected geometry were more stable. Therefore, the explorable region is maximized by choosing a system geometry that will slip before it will roll. We note that the spin rate of the sphere is rather large compared to most asteroids with rotation rates in the range 1 – 12 rev/day [13], but it is still within the observed range. Indeed, some monolithic asteroids have rotation speeds several times larger [12]. In such cases, exploration without use of gripping systems or thrusters is impossible with this mobility system.

IV. DYNAMIC ANALYSIS

In this section we study the crucial dynamical aspects for the operation of a hopping microgravity explorer: hopping initiation, ballistic flight, rebound dissipation, and instrument pointing.

A. Hopping Initiation

In this section, we intend to use first-order analysis techniques to demonstrate that the feasible trajectories for hopping rovers are almost exclusively defined by the contact force model. This, in turn, allows to draw several general conclusions about ideal rover design.

The rover behavior during actuation varies widely depending on the type of actuator used and on the command profile given to the actuator. While in contact with the ground, the rover can either be at rest on three or more contact points, pivot about an axis defined by one or more contact points without slipping, or rotate while the contact points slip. The following analysis captures all these possibilities. For clarity, linear actuation is considered separately from angular actuation.

1) *Equations of motion under linear actuation:* The governing equations in this case read as follows:

- 1) $\Sigma \vec{F}_{N_i} + \Sigma \vec{F}_{f_i} + m\vec{g} = m(\vec{\omega} \times \vec{\omega} \times \vec{r} + \vec{\alpha} \times \vec{r}) + \dot{\vec{p}}$,
- 2) $\|\Sigma \vec{F}_{f_i}\| / \|\Sigma \vec{F}_{N_i}\| \leq \min(\mu_s, \tan(\phi))$,
- 3) $\Sigma \vec{F}_N \cdot \hat{n} \geq 0$,

where $\dot{\vec{p}}$ is the time rate of change of the linear momentum of the actuator. In general, on a small body the rover should be operated at well below orbital speed. In addition, one seeks to maximize horizontal speed to increase size of the explored region, thereby improving the scientific return of the mission. Therefore, it is desirable to actuate the rover as quickly as possible using the lowest achievable trajectory. For simplicity, we consider the desired hopping speed of the rover to be some fraction of orbital speed. Accordingly,

a reasonable actuation model for linear systems would be: (1) the rover has a total mass m and an actuator mass m_a which can be moved a distance d in any direction; (2) the mass accelerates uniformly over its movable distance with an acceleration whose magnitude is a ; (3) the actuator mass collides inelastically and instantaneously with the wall of the rover; (4) the rover is on a region in which passive static equilibrium is possible; (5) the surface is locally flat; (6) the rover cannot roll during actuation; and (7) the rover is intended to move at some fraction c of local orbital velocity.

Under these assumptions, the speed of the rover is given by $v = m_a \sqrt{2ad}/m$ after actuation. Since the commanded velocity is a fraction of the orbital velocity, one obtains: $m_a \sqrt{2ad}/m = c \sqrt{gr}$. Hence, solving for the ratio of actuator force to gravitational force, $m_a a/mg$, one obtains:

$$m_a a/mg = c^2 m r / (2 m_a d).$$

It is reasonable to assume $c \geq 0.1$; also, typical values of r range between 100 m and 100 km for bodies of interest. It follows that $m_a a/mg \gg 1$ in most cases. Therefore, if the system is to develop speeds comparable to orbital speed, the actuating force vector dominates the behavior of the system. Therefore, we reasonably neglect the small terms in the governing force equation, leaving: $\Sigma \vec{F}_{N_i} + \Sigma \vec{F}_{f_i} = \dot{\vec{p}}$. Thus, according to the Coulomb friction model, an actuation force is achievable if its resulting contact forces satisfy the previous no-slip, no-roll, and no-grip conditions.

The above considerations give rise to the following conclusions regarding hopping initiation for internally-actuated rovers under linear actuation. For reliability, the actuator should be restricted to commanded forces that satisfy the aforementioned conditions or the rover will slide or roll, which may not be controllable. For ideal performance, the system should have a wide support base to allow the rover to achieve low hop angles (limited by static friction). To address viability, hop directional control is assured because no stipulations besides a minimum elevation are imposed on the actuator force. Additionally, moving at some fraction of orbital speed at a hop angle defined by the static friction coefficient is sufficient to achieve meaningful scientific information from exploration missions

2) *Equations of motion for angular systems:* In the same way, we make the following assumption for a “reasonable” actuation model under angular actuation (here, for simplicity, we consider a 2D model): (1) the rover has a mass m , an actuator moment of inertia j , a constant spike length l , and a remaining moment of inertia J ; (2) the rover applies a uniform torque T to the flywheel during actuation; (3) the rover is on a region in which passive static equilibrium is possible; (4) the surface is locally flat; (5) the rover does not slip during actuation; (6) the local gravity is normal to the surface; (7) the rover is intended to move at some fraction $c \geq 0.1$ of local orbital velocity.

Enforcing the non-slip constraint requires the following equations must be satisfied throughout the actuation process:

- 1) $T - m g l \sin(\psi) = (J + 1/2 m l^2) \ddot{\psi}$,
- 2) $F_N - m g = m l \ddot{\psi} \sin(\psi)$,

- 3) $F_f = m l \ddot{\psi} \cos(\psi)$,
- 4) $\|F_f\|/\|F_N\| \leq \mu_s$,
- 5) $g \geq \ddot{\psi}^2 l \cos(\psi)$,

where ψ defines the angle between the vector from the axis of rotation to the center of mass and the surface normal vector, as shown in Figure 3. The first three equations are required by Newton's 2nd law. The fourth equation is the Coulomb static friction condition, and the fifth equation is a constraint imposed by the non-slip assumption. The limiting case for the friction condition to be satisfied is then given by:

$$(l \ddot{\psi} \cos(\psi))/(l \ddot{\psi} \sin(\psi) + g) = \mu_s.$$

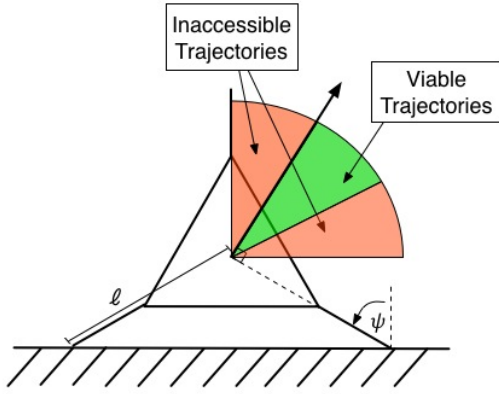


Fig. 3. Limitations on initial hopping angles for angular systems.

Again, the target velocity and gravity are related by the equation $v = c\sqrt{g\bar{r}}$, where the linear speed v is related to the rotation speed by $v = \dot{\psi}l$. As the rover rotates about the axes the angle between the velocity of the center of mass and the horizontal surface decreases. The maximum value of this angle, denoted ψ_0 (where $\psi_0 > 0$), is defined by the chosen geometry. Since the velocity vector cannot dip below horizontal and still cause the rover to hop, the center of mass of the rover follows a path no longer than $l\psi_0$. This requires an average linear acceleration of:

$$a = v^2/(2l\psi_0) = c^2 g r/(2l\psi_0).$$

Solving for a/g , one obtains $a/g = c^2 r/(2l\psi_0)$. Again, we assume that r ranges between 100 m and 100 km. Also, $l\psi_0$ is clearly on the order of meters or less. One then concludes that $a/g \gg 1$ in most cases. The result is again that the lowest hopping angle achievable is limited by the coefficient of static friction. Additionally, we must consider the consequences of the last condition. Since the target takeoff condition is $v = c\sqrt{g\bar{r}}$, one can eliminate g and obtain:

$$1 \geq c^2 r \cos(\psi)/l$$

Since r will exceed l by several orders of magnitude, this last condition cannot be satisfied at the target velocity. Consequently, the rover will either hop immediately at an angle of approximately ψ_0 , or start to slip. It is therefore

impossible to achieve hop angles larger than the greater of ψ_0 and $\arctan(\mu_k)$. Slipping takeoffs have simple dynamics since the direction of the contact force is defined by the kinetic friction coefficient. Consequentially, the slipping hop angle is *fixed* by the dynamic friction coefficient.

For geometries with large ψ_0 , we may achieve a larger hop angle envelope by implementing a more advanced control structure. One could apply a small torque to slowly adjust the attitude of the rover to the desired orientation, at which point the actuating torque is applied to initiate the hop. Such fine balancing attitude adjustment has been already demonstrated on the Cubli robot [8]. This strategy allows us to develop any hop angle between ψ_0 and the angle defined by the static friction coefficient as shown in Figure 3.

Finally, we consider the effect of local surface topology. Because the cone satisfying the static friction coefficient is defined by the surface norm vector, any change in the surface norm at the point of contact can substantially change the range of viable hop angles. This behavior is ignored in this analysis because it is entirely dependent on the local surface texture, which is largely unknown. Determination of the significance of these variances is left to future research.

This analysis has the following consequences for system design. On flat surfaces, rover geometries with large ψ_0 (fewer faces) will perform well so long as attitude control is implemented in the actuation method. Conversely, geometries with low ψ_0 values will always slip when hopping, resulting in a *fixed* hop angle. In addition, the chosen geometry imposes an upper limit to the hop angle, which may be problematic if the rover were to fall in a hole. There are no limitations on the hop direction and the horizontal speed limitations are identical to those of linear systems, which demonstrates viability of using angular actuators to achieve hopping.

B. Analysis of Flight Regime

In this section, we briefly study ballistic flight on a rotating body in order to characterize the impact of the Coriolis effect on the ballistic trajectories and defend the assumption of target speed being a fraction of orbital speed. The Coriolis acceleration, a_{cor} , is given by $a_{cor} = 2m(\vec{\omega} \times \vec{v})$, where \vec{v} is the velocity of the rover in flight. Under the previous assumption that the hop speed is a fraction c of the orbital speed, the worst-case magnitude of the Coriolis acceleration is $a_{cor} = 2\omega c\sqrt{g\bar{r}}$. Using previously established ranges for c , ω , and r , one concludes that $a_{cor} \ll g$ in most cases. The consequence of this analysis is that if the Coriolis effect is only a minor consideration in motion planning. Following this, the assumption of traveling at the previously discussed fraction of orbital speed is within reason.

C. Rebound dissipation

A critical aspect of the operation of hopping rovers is to maximize kinetic energy dissipation in order to minimize uncontrolled bouncing and tumbling. In this section we propose methods for efficiently damping these modes.

1) *Bouncing Dissipation*: When a rover is first landing from a hop, it will tend to bounce and tumble in an uncontrolled manner. One possible strategy to minimize this behavior is similar to the function of a dead blow mallet. We propose that the actuator system be mounted in a hollow shell containing sand or other loose material. This system is illustrated in Figure 4.

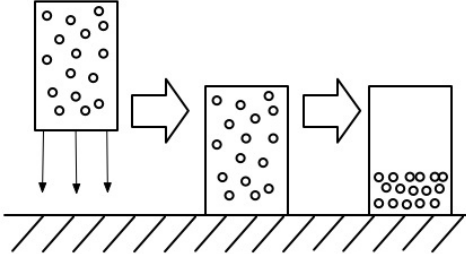


Fig. 4. A possible strategy to mitigate residual bounces, inspired by the function of a dead blow mallet.

In flight, the material will distribute itself evenly in the shell. When the system lands, the shell will rebound immediately, but the sand will continue to fall into the bottom of the shell as a continuous inelastic collision. Thus, the sand effectively reduces the coefficient of restitution, increasing energy dissipation. This behavior is independent of the magnitude of the kinetic energy of the system. A first order analysis is conducted under the following assumptions: (1) the rover has a shell mass m_{shell} and an additional mass of particulate material m_{sand} ; (2) upon impact with the ground, the shell rebounds instantaneously with a coefficient of restitution e ; (3) the shell undergoes a perfect inelastic collision with the particulate matter.

Our goal is to determine what effect the particulate will have on the observed coefficient of restitution of the total system. Combining the equations for these two collisions yields and solving for the effective restitution coefficient, e_{eff} , read as:

$$e_{eff} = \max\left(\frac{e - m_{sand}/m_{shell}}{1 + m_{sand}/m_{shell}}, 0\right).$$

If a linear actuator is used, the actuator mass can be used instead of the loose particulate, decreasing the total mass of the system. This application has been previously studied in [15]. The analysis presented in [15] agrees with the first order analysis at the limit case ($m_{sand}/m_{shell} = 1$), which prevents any vertical rebound.

2) *Wobbling Dissipation*: In this section we propose a method to quickly dissipate energy in rolling and wobbling modes. When a rover is landing after a hop and the remaining energy is insufficient to cause the rover to bounce, the rover may still roll or wobble before finally coming to rest on a face, increasing the time between hops. The dynamics of this motion are similar to those of the rimless wheel [16]. The work [16] presents a 2-D analysis that uses conservation of angular momentum to determine the energy dissipation.

Generalizing this model to 3-D, geometries satisfying the condition that the angles spanned by vertices or edges exceed 90 degrees should not rebound at all when rolling or wobbling. This suggests that using a geometry with few faces, such as a cube or tetrahedron, would effectively eliminate rolling or wobbling modes. However, because the time constant for wobbling motion in milli- to microgravity environments is orders of magnitude higher than in Earth gravity, any errors in this model may introduce significant time delays.

To maximize energy dissipation in these modes, we propose that a flexible casing of small spheres be fixed to the end of the spikes, much like a Hacky Sack. When a spike comes into contact with the ground, the spheres would slide inside the casing, absorbing the impact energy without developing an elastic compression, preventing the spike from rebounding. Because the kinetic energy of the rover is not likely to exceed the order of mJ, these cases can be made very small and still easily be able to dissipate all kinetic energy in the system. This system would effectively make the rover behave as if it were landing on loose material regardless of the surface characteristics. This is a highly desirable behavior since loose materials are known from observation to have excellent dissipation characteristics. Such a system would also give each spike a larger contact area, which may be necessary to avoid sinking into sand or dust.

D. Instrument Pointing

Scientific missions to small bodies will entail repeated use of scientific instruments to characterize the surface. Mobility systems must be able to reliably point these instruments to meet mission requirements. In this section we analyze the feasibility of each type of actuator system to meet these requirements.

1) *Linear systems*: Attitude adjustment for systems using linear actuators is a nontrivial problem. A common method used for these systems is to use the actuator to shift the center of mass, causing the rover to roll. We will now demonstrate that the geometric requirements for this implementation and the aforementioned ideal geometry for low takeoff angles are in *direct contradiction* through 2-D analysis. To achieve rolling, one must displace the center of gravity over the edge of the support region. Let the ensemble of spikes form a regular polygon with n vertices and length l from the center to each vertex. The internal angle spanned by each side is $2\pi/n$ radians. Now let us assume the system is composed of two masses, the shell mass m_s located at the center, and the actuator mass m_a that can be placed anywhere within the polygon. To roll, we require the center of mass of the system to be over the edge of the support face. Assuming that the actuator mass can be moved a distance l from the center of mass (a slight simplification), the required mass ratio to move the center of mass a distance $l \sin(\pi/2)$ follows the relation $m_a/m_s \geq \sin(\pi/n)/(1 - \sin(\pi/n))$ when $n > 4$. Because we already established that minimizing the number of faces is a design priority, using this system would clearly compromise system performance. On the other hand, if a

system with a single actuator with an orientation mechanism is used, the orientation system can be used to control attitude adjustment.

2) *Angular systems*: Fine attitude adjustment for torque actuated systems has already been demonstrated by the Cubli robot [8] in Earth gravity. This technique would easily satisfy the instrument pointing requirement. Additionally, it is possible to achieve instrument pointing in regions where the rover would roll without active control. In such cases the actuator torque can be set to directly oppose the gravitational torque, though this is only sustainable until the flywheel motor reaches its saturation speed. Furthermore, it is possible to maneuver on these surfaces by small adjustments of the torque to achieve controlled rolling motion. If the rover is traveling downhill, minimal torque will be needed since the behavior will be similar to that of a rimless wheel [16], which is known to have a stable rolling speed. Uphill rolling can be achieved by applying a constant torque only slightly higher than the gravitational torque. It is important to note that this motion would be restricted to rolling in a straight line to avoid introducing gyroscopic effects from the flywheels. Using a reference gravitational acceleration of 1 mm/s^2 and current specifications for the Hedgehog rover [3], which includes a mass of 10 kg , a leg length of 0.3 m , a flywheel moment of inertia of $0.02 \text{ kg} \cdot \text{m}^2$ and a saturation speed of 1000 rad/s , simple Buckingham Pi analysis suggests that the rover could hold the maximum gravitational torque for over 6000 s . The conservative nature of this method suggests that the time limit is actually much higher. This control system would allow an angular actuator system to maintain pointing in any region where the contact force is consistent with Coulomb friction even if the rover would roll with no active control. This is as versatile as any system without gripping or thruster capability.

V. ANALYSIS FOR REFERENCE MISSION TO PHOBOS

In this section, we demonstrate a full analysis of a reference mission to Phobos as outlined in [3] to demonstrate that internally actuated systems are a feasible option for exploration missions to small bodies.

The difference between this procedure and the static analysis is the condition to allow the motor to apply a minimum torque, T_{min} , to spin up the flywheel, which reads as:

$$F_n l \left(\sin(\theta) - F_f / \|E_n + F_f\| \right) \geq T_{min}.$$

This condition requires that the line of action of the contact force be sufficiently far from the edge of the polygon of support to allow the flywheel to spin up without the rover rolling. It is important to note that this equation imposes a directional sensitivity to the analysis (i.e. the rover may still be able to actuate in some directions). For simplicity, in this method we require that this condition be satisfied in all directions.

To demonstrate the consequences and relevance of this analysis, we consider the reference mission proposed in [3]. The gravity field is calculated using the previously described

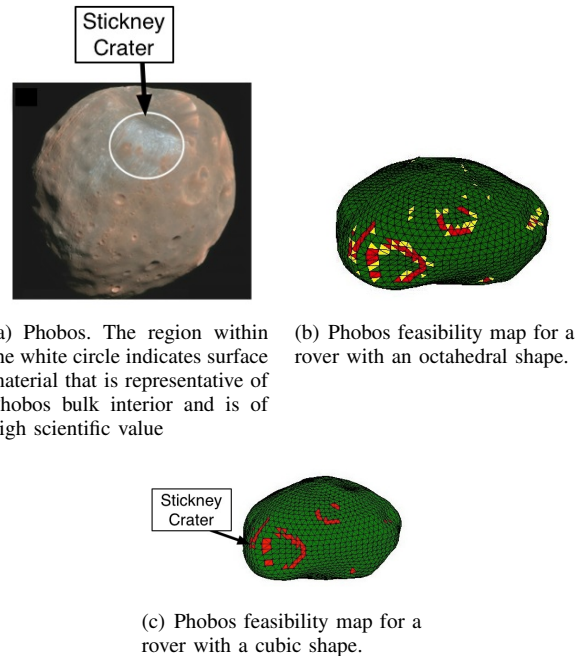


Fig. 5. Dynamical feasibility map for the Hedgehog rover on Phobos as a function of its spikes' geometrical envelope.

method, and we assume a static friction coefficient of 0.7 . The rover has a mass of 10 kg and spike length of 0.2 m . We assume a motor torque resolution of $1 \text{ mN} \cdot \text{m}$. Lastly, we consider octagonal and cubic shapes. The results of these studies are shown in Figures 5(b) and 5(c). The yellow regions present in Figure 5(b) indicate regions where the spin-up restriction prevents the rover from actuating correctly. Note that the cube geometry eliminates these regions due to increased stability. To further demonstrate the viability of these systems, we show summary results from analysis of the a cubic rover with no minimum torque requirement on bodies of scientific interest in Table I. We acknowledge a degree of uncertainty in these calculations due to the dependence on the accuracy of the shape models.

TABLE I
EXPLORABLE REGIONS FOR A SET OF REPRESENTATIVE TARGETS.

Body Name	Mass (kg)	Period (h)	Explorable Regions
Phobos	$1.072 \cdot 10^{16}$	7.66	97%
Deimos	$1.48 \cdot 10^{15}$	30.3	96%
Itokawa	$3.51 \cdot 10^{10}$	12.1	75%
Hartley 2	$4.7 \cdot 10^{11}$	18.3	99%

VI. DISCUSSION AND CONCLUSIONS

In this paper we have studied the “dynamic envelope” of hopping microgravity rovers, with a focus on internal actuation. Our findings are summarized below together with a discussion about directions for future research.

A. Viability Demonstration

This analysis has shown that internally actuated systems are a viable option for exploration missions to small bodies of scientific interest. In Section IV-A, we demonstrated that internally actuated systems are sufficiently mobile to meet the needs of exploration missions. In Section IV-B, we demonstrated that the Coriolis effect will not significantly affect the flight path. In Section IV-C we discussed methods to minimize uncontrolled tumbling upon landing. Although the time scale of this behavior are still slow, they can be reduced to insignificant levels compared to the mission timescale (e.g. rotation period) with such dissipation systems. Lastly, we showed that Phobos and many other bodies of scientific interest meet the aforementioned requirements.

1) *Linear Actuator Systems:* Linear actuator systems are restricted to regions where the contact force satisfies the contact force model and the no-roll condition with no active control. Controlling the hop angle is very simple with these systems so long as the change in contact force is consistent with the contact force model and the no-roll condition. While the rover will have better hopping behavior if a wide support base is used, meeting the instrument pointing requirement would be more difficult. Using a single linear actuator on a rotating frame can alleviate this problem since the frame control can be used to meet the pointing requirement.

2) *Angular Actuator Systems:* When using an angular actuator, the system can explore any region where the required contact force is possible so long as the aforementioned controls are implemented. The only way to improve this performance is to include a gripping or thruster system. The hop angle for these systems have an upper limit defined by the geometry of the system, which may be problematic if the rover falls into a hole. Using a wide support base increases this upper limit and reduces the need for active control to prevent rolling.

B. Future Work

Recognizing that this analysis depends strongly on the contact force model, efforts to characterize the contact force behavior of regolith and loose material surfaces is warranted. For exploration missions to be successful, it is essential to have functional contact force models for these surfaces in order to determine any further mobility restrictions. To achieve this, we plan to perform an experimental validation of these conclusions on these surface types.

This analysis has direct consequences to the path planning process for exploration missions, which represents an important future research avenue. The dynamic environment introduces a number of complications in this process. The existence of regions in which rovers cannot achieve static equilibrium requires path planning algorithms capable of identifying and avoiding such regions. These regions may vary with time on tumbling bodies due to the explicit dependence on angular velocity and acceleration. Use of the aforementioned slow spin-up procedure or active stabilization controls on slopes introduces directional mobility restrictions, making determination of feasible paths more

difficult. Path planning algorithms for these missions must account for all of these limitations. The numerical method for determination of explorable regions presented in this paper can already account for most of these restrictions, and could easily be modified to identify the rest of these constraints. This method may be developed into a path planning system in the future.

REFERENCES

- [1] Decadal Survey Vision and Voyages for Planetary Science in the Decade 2013–2022. Technical report, National Research Council, 2011. Available at <http://solarsystem.nasa.gov/2013decadal/>.
- [2] JAXA Hayabusa mission. Technical report, JAXA, 2011. Available at <http://hayabusa.jaxa.jp/e/index.html>.
- [3] R. Allen, M. Pavone, and C. McQuin. Internally-actuated rovers for all-access surface mobility: Theory and experimentation. In *Proc. IEEE Conf. on Robotics and Automation*, May 2013.
- [4] J. Bellerose and D. Scheeres. Dynamics and Control for Surface Exploration of Small Bodies. In *AIAA/AAS Astrodynamics Specialist Conference and Exhibit*, Honolulu, HI, August 2008.
- [5] J. C. Castillo-Rogez, M. Pavone, I.A.D. Nesnas, and J.A. Hoffman. Expected science return of spatially-extended in-situ exploration at small Solar System bodies. In *Aerospace Conference, 2012 IEEE*, pages 1–15, March 2012.
- [6] C. Dietze, S. Herrmann, F. Kuß, C. Lange, M. Scharringhausen, L. Witte, T. van Zoest, and H. Yano. Landing and mobility concept for the small asteroid lander MASCOT on asteroid 1999 JU3. In *61st International Astronautical Congress*, 2010.
- [7] P. Fiorini and J. Burdick. The development of hopping capabilities for small robots. *Autonomous Robots*, pages 239–254, 2003.
- [8] M. Gajamohan, M. Merz, I. Thommen, and R. D’Andrea. The Cubli: A cube that can jump up and balance. *2012 IEEE/RSJ International Conference on Intelligent Robots and Systems*, pages 3722–3727, October 2012.
- [9] V. Guibout and D. J. Scheeres. Stability of Surface Motion on a Rotating Ellipsoid. *Celestial Mechanics and Dynamical Astronomy*, 87(3):263–290, November 2003.
- [10] R.M. Jones. The MUSES–CN rover and asteroid exploration mission. In *22nd International Symposium on Space Technology and Science*, pages 2403–2410, 2000.
- [11] M. Pavone and J.C. Castillo-Rogez. Spacecraft/Rover Hybrids for the Exploration of Small Solar System Bodies. *IEEE ...*, 2013.
- [12] P. Pravec. Fast and Slow Rotation of Asteroids. *Icarus*, 148(1):12–20, November 2000.
- [13] P. Pravec, A.W. Harris, D. Vokrouhlický, B.D. Warner, P. Kušnirák, K. Hornoch, D.P. Pray, D. Higgins, J. Oey, A. Galád, Š. Gajdoš, L. Kornoš, J. Világi, M. Husárik, Yu.N. Krugly, V. Shevchenko, V. Chorny, N. Gaftonyuk, W.R. Cooney, J. Gross, D. Terrell, R.D. Stephens, R. Dyvig, V. Reddy, J.G. Ries, F. Colas, J. Lecacheux, R. Durkee, G. Masi, R.A. Koff, and R. Goncalves. Spin rate distribution of small asteroids. *Icarus*, 197(2):497–504, October 2008.
- [14] R.Z. Sagdeev and A.V. Zakharov. Brief history of the Phobos mission. *Nature*, 341:581–585, 1989.
- [15] S. Shimoda, T. Kubota, and I. Nakatani. New mechanism of attitude control for hopping robot. *IEEE/RSJ International Conference on Intelligent Robots and System*, 3:2631–2636, 2002.
- [16] R. L. Tetrake. *Applied optimal control for dynamically stable legged locomotion*. PhD thesis, Massachusetts Institute of Technology, 2004.
- [17] S. Ulamec, V. Kucherenko, J. Biele, A. Bogatchev, A. Makurin, and S. Matrossov. Hopper concepts for small body landers. *Advances in Space Research*, 47(3):428–439, February 2011.
- [18] M. Wargo. Strategic knowledge gaps. 2012. Available at http://science.nasa.gov/media/medialibrary/2012/05/04/HEOMD_Strategic_Knowledge_Gaps_--_Mike_Wargo.pdf.
- [19] T. Yoshimitsu, T. Kubota, I. Nakatani, T. Adachi, and H. Saito. Micro-hopping robot for asteroid exploration. *Acta Astronautica*, 52(2-6):441–446, January 2003.
- [20] T. Yoshimitsu, I. Nakatani, and T. Kubota. New Mobility System for Small Planetary Body Exploration. In *Proc. IEEE Conf. on Robotics and Automation*, pages 1404–1409, May 1999.